J Bionic Eng 17 (2020) 932–943
DOI: https://doi.org/10.1007/s42235-020-0090-8

Journal of Bionic Engineering
http://www.springer.com/journal/42235

Design and Fabrication of a Multi-motion Mode Soft Crawling Robot

Youxu Chen[1,2], Bingbing Hu[1,2], Jiakang Zou[1,2], Wei Zhang[1,2], Deshan Wang[2], Guoqing Jin[1,2*]

1. *Robotics and Microsystems Center*, *Soochow University*, *Suzhou* 215006, *China*
2. *School of Mechanical and Electric Engineering*, *Soochow University*, *Suzhou* 215006, *China*

Abstract

This article proposes a novel pneumatic soft actuator, which can perform bending in different directions under positive or negative air pressure. The actuators are composed of multiple airbags, and the design of the airbags is analyzed. A pneumatic soft robot based on these soft actuators is designed and fabricated by 3D printing technology. This robot consists of three soft multi-bladder actuators, one soft sensor, middle layer, bottom layer, front barb, front feet and rear feet. According to the different positive or negative pressure control of the three soft multi-bladder actuators, the robot can perform both linear, crossing and climbing movements. The soft robot has excellent environmental adaptability and can pass through complex environments by combining three modes of motion. Then, we establish the closed-loop automatic control system using soft sensor. The soft sensor can be stretched and compressed as the soft robot's movement. Finally, the automatic control system is verified by linear, crossing and climbing movement experiments. Results indicate that the robot can pass through complex environments under the closed-loop control system.

Keywords: soft multi-bladder actuator, 3D printing, soft robot, soft sensor

1 Introduction

Nature has long been the source of inspiration to make new kind of machines. Learning from the soft and body compliance of creatures, a new class of machine, called soft robot, has been developed, which is now the hot spot and development frontier of robotics. Compared with traditional rigid robots, the soft robots show good environment adaptability and human-machine interactivity. They can adjust their structures to adapt to environment changes, and can be applied in the fields of military, scientific research and medical treatment in the future. At the moment, most of the bionic soft robots are designed to adapt to the complex and varied natural environment[1,2].

The soft crawling robot is one of the main research directions of soft robots. Many soft crawling robots are capable of performing both linear and turning movements, and some even have the ability of jumping, rolling, and swimming[3,4]. Inspired by nature, scientists have studied and designed a series of soft crawling robots in the last decade[5,6]. At present, the soft crawling robots can be driven by different driving modes, such as pneumatics[7], dielectric elastomer[8], ionic polymer metal composite, Shape Memory Alloy (SMA)[9], and responsive hydrogel[10]. Umedachi *et al*. designed a soft crawling robot based on a 3D printed shell and an embedded SMA actuator by studying caterpillar movement[11]. Wang *et al*. designed a crawl robot imitating the inchworm[12]. The soft robot can crawling and turning by equipping a memory alloy. Shepherd *et al*. developed a multi-gait soft robot[13], which was fabricated by soft lithography and was pneumatically actuated, capable of sophisticated locomotion. Guo *et al*. designed an inchworm-like soft robot with omega-arching locomotion and driven by pneumatics[14], which is mimic the circular and longitudinal muscles to perform telescopic locomotion. Hu and Jin designed a multi-actuator soft robot based on the detailed morphological and kinematic investigations of the young tiger beetle, which can achieve the crawling, steering and occluding movement by pneumatics[15]. Duduta *et al*. designed a crawling soft robots based on dielectric elastomer actuators, which is created by a multilayer fabrication method[16]. Nakamaru *et al*. designed a crawling soft robot driven by a novel self-oscillating gel actuator[17]. Shi *et al*. designed a crawling soft robot controlled by a SMA wire[18].

The above soft crawling robots are driven by dif-

***Corresponding author:** Guoqing Jin
E-mail: gqjin@suda.edu.cn

ferent actuators, and they only have one mode of movement, crawling on flat ground, shown in Fig. 1a. Fig. 1b shows the principle of the soft robots crawling on a flat ground. In order to achieve crawling on the complex ground, we designed a multi-motion modes soft robot, and the crawling principle is shown in Fig. 1c. The body structure of the soft robot is directly printed on the 3D printing platform by the silicone rubber material. Under the control of the closed-loop system, it can adaptively complete linear crawling movements, crossing movements on obstacles and climbing movements on step surfaces in complex environments.

The actuators are composed of multiple airbags, and the design of the airbags is analyzed. In order to analyze the motion characteristics of the soft actuator, the theoretical analysis model between air pressure with deflection angle and the simulation analysis of soft actuator are established. Then we design a multi-motion modes soft crawling robot inspired by the inchworm's movement pattern. This robot consists of three soft multi-bladder actuators, soft sensor, middle layer, bottom layer, front barb, front feet, and rear feet. The soft crawling robot has multi-motion modes, which can perform linear movement in flat ground, crossing movement in obstacle environment and climbing movement mode in step environment, according to the different control patterns. The three control patterns will be presented late. Because the soft actuator can forward bending and reverse bending, it can cross the obstacles according to the different air pressure. Because of its soft structure, it has the potential to be applied to the complex natural environments. To realize the automatic control of this soft crawling robot, we establish the pneumatic control platform based on the soft sensor. Finally, the ability of soft crawling robot to move in complex environments is verified by experiments of linear, crossing and climbing movements.

2 Methodology

2.1 The design of actuator

2.1.1 The design of different multi-airbags

At present, most soft robots are made up of pneumatic soft actuators, which are composed of rectangular cavity multi-airbags. The bending of the actuator is caused by inflating and deflating the airbags. When the soft actuator is inflated, due to the expansion of each air bag, the soft actuator generates the down warping. However, due to the limitation of the rectangular cavity of the airbag, the soft actuator can only bend downward. To allow the soft actuator to bend upward on inhalation, we changed the rectangular cavity to a trapezoidal cavity (Fig. 2). The new soft actuator of trapezoidal cavity multi-airbags can bend downward under positive pressure and upward under negative pressure.

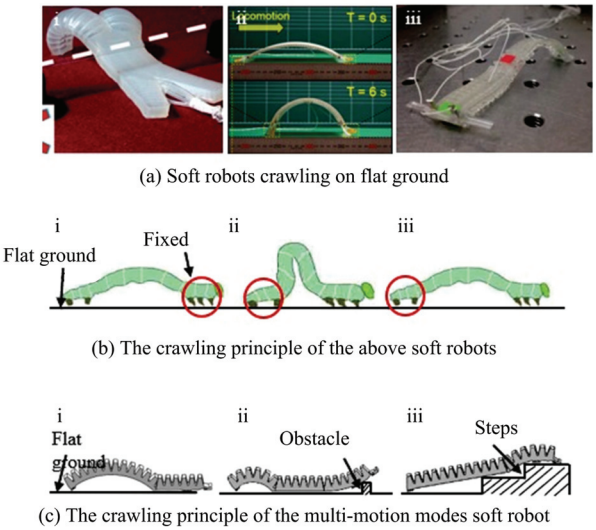

(a) Soft robots crawling on flat ground

(b) The crawling principle of the above soft robots

(c) The crawling principle of the multi-motion modes soft robot

Fig. 1 Comparison of performance and crawling principle between the multi-motion modes soft robot and previous soft robots.

2.1.2 The simulate of the soft actuator

To verify the bending ability of the soft actuator, a finite element simulation is carried out. In this paper, Abaqus software is used to simulate and analyze the multi-airbag soft actuator of rectangular cavity. Abaqus is a professional simulation software that is applicable to non-linear analysis. It can carry out gas-solid coupling simulation analysis on the soft actuator and analyze the deformation under different pressures. The multi-airbag soft actuator is made of silicon rubber. The material used in this paper was a clear, one-part oxime cure silicone rubber (Dow Corning® 737) with density of 1.04 g·cm^{-3} and the viscosity of 62.5 Pa·s. It cures upon exposure to atmospheric moisture and features a durometer hardness of Shore 33A, a skin-over time of 3 min to 6 min, a tack-free time of 14 min, and a cure to handling time of 24 h[21].

Reduced N-order silicone material models repre-

sented by Eq. (1) were used to fit the tensile test data for the silicone materials where the material was considered incompressible and the strain energy potential U is independent of the second invariant[22]:

$$U = \sum_{i=1}^{N} C_{10} \left(I_1 - 3\right)^i, \quad (1)$$

I_1 is the first deviatoric strain invariant and C_{ij} is a material specific parameter. The Ogden model ($N = 3$) was also investigated, represented by Eq. (2) for the strain energy potential U as a function of deviatoric principal stretches λ_i and is represented by the following relation for incompressible materials:

$$U = \sum_{i=1}^{N} \frac{2u_i}{a_i^2}\left(\lambda_1^{a_1} + \lambda_2^{a_2} + \lambda_3^{a_3} - 3\right) + \sum_{i=1}^{N} \frac{1}{D_i}\left(J-1\right)^{2i}, \quad (2)$$

where u_i and a_i are empirical parameters. The constitutive equation Ogden was used to describe the properties of silicon rubber during the analysis and the model parameters are shown in Table 1[20].

The Finite Element Analysis (FEA) of the soft actuator is carried out in the case of ignoring the frictional force and gravity, and the positive and negative pressures of different sizes are filled in the air cavity. As shown in Fig. 3a, the soft actuator can be bent downward through expansion deformation under positive pressure. As shown in Fig. 3b, the soft actuator can be bent upward through contraction deformation under negative pressure.

2.1.3 The design of the trapezoidal cavity multi-airbags

The multi-airbags actuator is made of cast silicon rubber material, and we adopted the Yeoh model to describe the mechanical properties of the soft actuator[19,20]. Base on the constitutive relation of rubber materials of Yeoh model, we adopted the E to describe the strain energy density function:

$$E = C_1\left(I_1 - 3\right) + C_2\left(I_2 - 3\right)^2, \quad (3)$$

$$\boldsymbol{W} = \left(\boldsymbol{I} + \frac{\partial(v)}{\partial(x,y,z)}\right)\left(\boldsymbol{I} + \frac{\partial(v)}{\partial(x,y,z)}\right)^{\mathrm{T}}, \quad (4)$$

where C_1 and C_2 are the material constants[20]. l_1 and l_2 are the strain in variants. $l_1 = l_2 = tr\,(w)$, w is the Cauchy green strain tensor. $\boldsymbol{I}$ is the identity matrix, v is the displacement of the airbag's inflated and inhaled wall

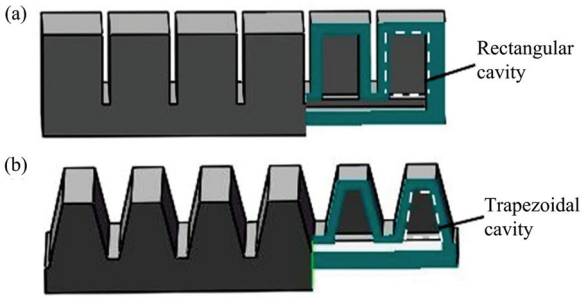

Fig. 2 Different multi-airbags soft actuators. (a) Rectangular cavity soft actuator; (b) trapezoidal cavity soft actuator.

Table 1 The parameters of Ogden model[20]

Constitutive equation	Coefficient u_i	Coefficient a_i	Coefficient D_i
Ogden $N = 3$	$u_1 = 2.3461\times10^{-2}$	$a_1 = 1.7183$	$D_1 = 3.2587$
	$u_2 = 6.6703\times10^{-5}$	$a_2 = 7.0679$	$D_2 = 0$
	$u_3 = 4.5381\times10^{-4}$	$a_3 = -3.3659$	$D_3 = 0$

which is $v = (v_x, v_y, v_z)$. To get the displacement of any point in the inflated and inhaled wall, we study two airbags of the soft actuator. In Fig. 4, where h is the height of the wall, k is the width of the wall, d is the thickness of the wall, s is the width between two airbags, g is the width of the airbags, a_1 is the maximum displacement of the airbag's inflated wall, and a_2 is the maximum displacement of the airbag's inhaled wall. Since the silicone material is incompressible, it is assumed that there is no deformation in the width direction when the soft actuator is inflated or inhaled. We assume the coordinate of any point on the wall is (x, y, z), and after inflating or inhaling the point can be expressed as (x', y', z'):

$$\left(x', y', z'\right) = \left(x + af\left(\frac{z}{h}\right)f\left(\frac{y}{k}\right), y, z\right), \quad (5)$$

where $f(x)$ is the monotonically decreasing function, and the range of $f(x)$ is between 0 and 1. So we can assume the function $f(x) = 1 - x^2$. The function $f(x)$ satisfies the following conditions:

$$f(0) = 1, \quad f(1) = 0, \quad f(0)' = 0. \quad (6)$$

By simplifying, we can get the following equation:

$$\left(v_x, v_y, v_z\right) = \left(af\left(\frac{z}{h}\right)f\left(\frac{y}{k}\right)0, 0\right), \quad (7)$$

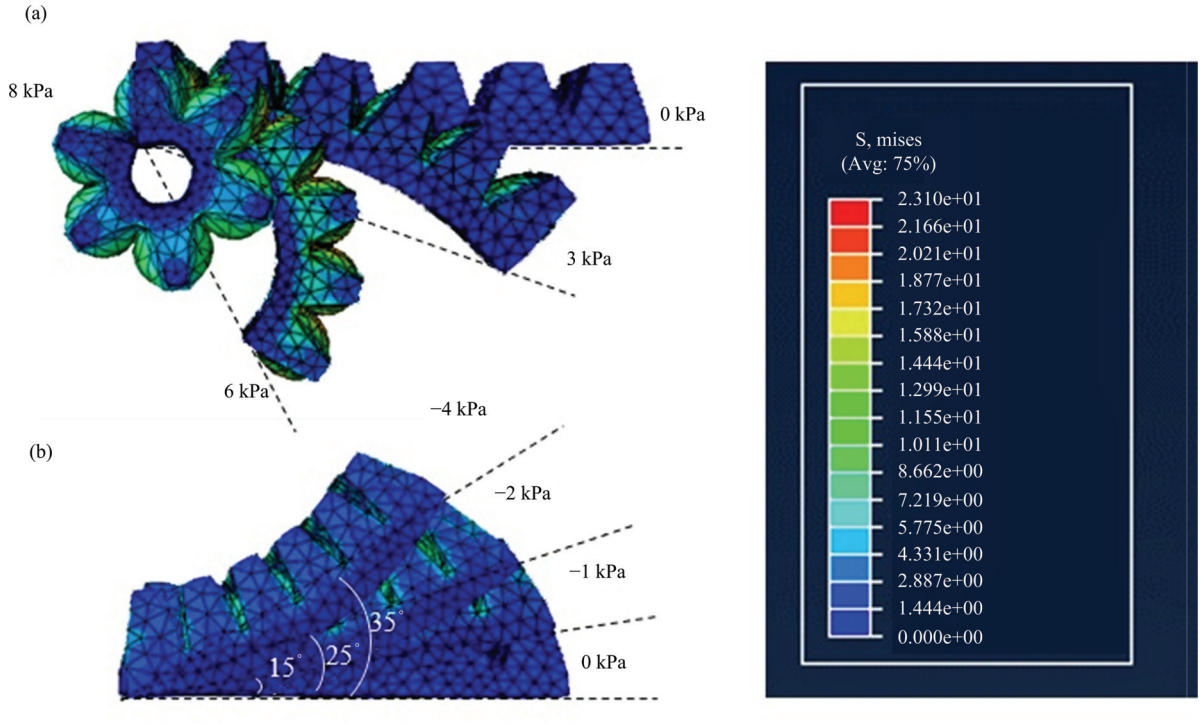

Fig. 3 The simulate results of the soft actuator. (a) Expansion and bending deformation at 0 kPa, 3 kPa, 6 kPa and 8 kPa; (b) shrinkage deformation bending at 0 kPa, −1 kPa, −2 kPa and −4 kPa.

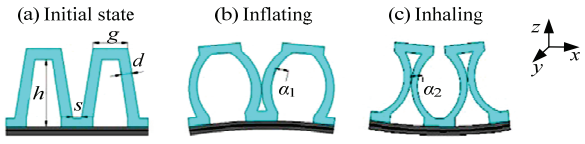

Fig. 4 Cross section of two airbags in three separate states.

$$E = C_1\left[\frac{2048}{1575}\left(\frac{h^2}{k^2}+\frac{k^2}{h^2}\right)+\frac{2048}{11025}\right]\frac{a^4 d}{hk}+ C_2\frac{32}{45}\left(\frac{h}{k}+\frac{k}{h}\right)a^2 d. \tag{8}$$

Base on the virtual work principle, we can calculate the functional relationship between the deformation a and air chamber's pressure p. The strain energy of the inflated or inhaled wall equals to the work of the pressure along the displacement of the X-axis:

$$\frac{\mathrm{d}E(a)}{\mathrm{d}a}\delta a = p\frac{\mathrm{d}v(a)}{\mathrm{d}a}\delta a, \tag{9}$$

$$v(a) = ahg_0^1 f(x)\mathrm{d}x, \tag{10}$$

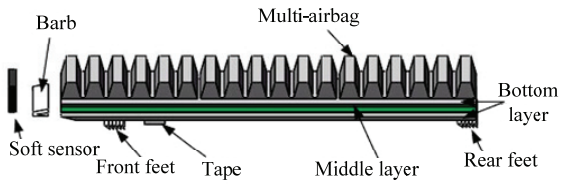

Fig. 5 The explosive view of multi-motion modes soft crawling robot.

$$p = C_1\left[\frac{6144}{525}\left(\frac{h^2}{k^2}+\frac{k^2}{h^2}\right)+\frac{6144}{3675}\right]\frac{a^3 d}{h^2 k^2}, \tag{11}$$

where g_0^1 represents the acceleration of gravity. Based on the Eq. (11), we can find the deformation increased with the pressure p, and the deformation a decreased with the airbag wall d under fixed pressure p.

2.2 The design of the soft robot

2.1.1 The design of the multi-motion modes soft crawling robot

The soft crawling robot consists of two parts, head and body. The body consists of three soft multi-bladder actuators, middle layer, bottom layer, front barb, front

feet, and rear feet. As shown in Fig. 5, the multi-bladder actuator consists of multi-airbags, a middle layer and a bottom layer. The soft actuator is made of silicone rubber. In Fig. 6, the function of the middle layer is to prevent the expanding of the base board and enhance the resilience, so it is made of no ductile flexible materials, such as PVC slice. The trapezoidal cavity structure of the airbags is different from the traditional rectangular cavity structure. As shown in Fig. 4, the airbags can be bent downward by expansion deformation under positive pressure, while bent upward by contraction deformation under negative pressure. The front and rear feet are used as anchors when the soft robot's body making a movement. But when the soft robot's head makes a linear movement, the front barb and rear feet are used as anchors. The front barb is made of the rigid barbed structure, and the front and rear feet are a raised barb structure made of silicone rubber.

The multi-motion modes soft crawling robot contains three columns of multi-airbags, and each column is an actuator. There are 6 airbags in one actuator. Each trapezoidal airbag of one actuator is connected by the gas slot which is in the bottom of the airbags. There are three tubes, and each tube is inserted into the middle airbag of the actuator. While inflating, the gas flows through the tubes and reaches the middle airbag of the actuator. Due to the expansion of each air bag, the soft actuator generates the down warping motion. A PVC slice is embedded in the bottom plate of the soft robot to take advantage of the inextensibility of the PVC sliceto limit the expansion during inflation of the airbag, and thus produces a bending down movement. While inhaling, the air in the multi-airbag will be drawn out. Due to the shrink of each air bag, the soft actuator generates the up warping.

2.2.2 The design of the soft sensor

In order to realize the closed-loop control of the soft crawling robot, a custom soft triboelectric tactile sensor is designed. The tactile sensor is used to judge whether the robot touches obstacle or not. It is an important medium for the robot to perceive the external environment and perceive the proximity between the robot and the surrounding obstacles.

The soft tactile sensor is made of silicone rubber and liquid metal. Silicon rubber is a kind of tribological electronegativity material with excellent electronic affinity and tensile deformation ability, and it is quite fit for making software sensors. Liquid metal has excellent conductivity, taking liquid metal as the electrode, it has a good deformation ability while maintaining good conductivity.

The working principle of the soft triboelectric tactile sensor is shown in the Fig. 6. In Fig. 6a, the electrons move from the obstacle surface to the silicone surface when the obstacle comes into contact with the triboelectric tactile sensor. In Fig. 6b, when the obstacle leaves, two surfaces with opposite charges separate and produce a potential difference, current and voltage output. In Fig. 6c, the electron stops moving and achieves static equilibrium when the obstacle is far away. In Fig. 6d, the reverse electrons flow from the ground to the

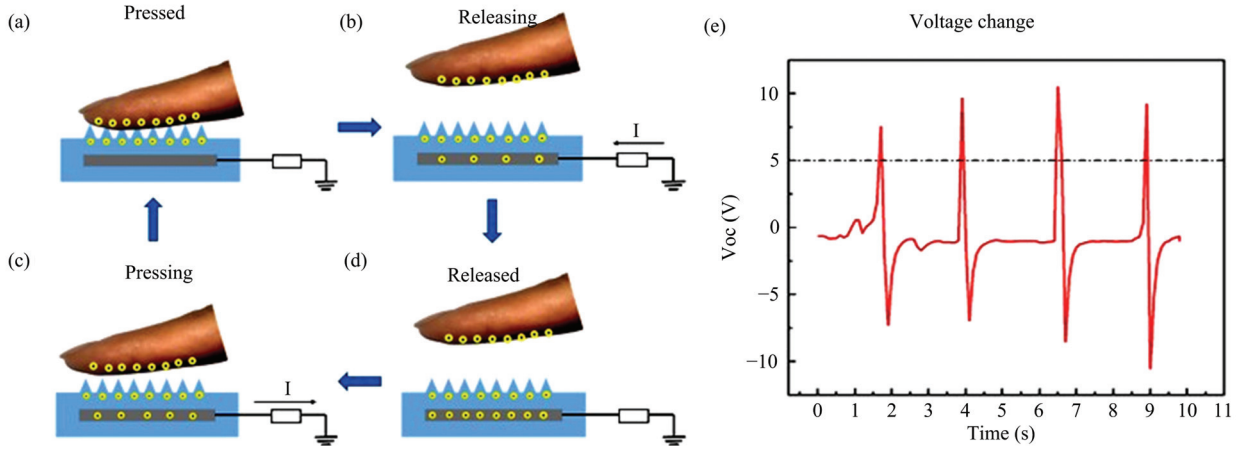

Fig. 6 (a–d) The working principle and (e) the voltage change of the soft triboelectric tactile sensor in the process of contacting obstacles.

electrode and generate voltage in the opposite direction when the obstacle approaches again.

As shown in Fig. 6e, it shows the voltage change of the soft triboelectric tactile sensor in the process of contacting obstacles. One of these cycles represents a contact separation process between the tactile sensor and the obstacle. In the closed-loop control system, we set the voltage of 5 V as the threshold voltage. When the voltage of the sensor reaches this value, the controller controls the solenoid valve to open periodically.

2.3 Fabrication process

2.3.1 Materials

The list of material used in multi-motion modes soft robot consists of silicone rubber (Dow Corning 737, Eco-flex 0050), silicone air tube, polylactic acid (PLA), rigid barb, PVC slice, liquid metal. The silicone rubber is a hyperplastic and soft rubber with a small Young's modulus (65 kPa) and large Poisson's ratio (0.49), it can stretch easily and recover the original shape repeatedly. The silicone rubber Eco-flex 0050 was mixed and curing agent in a 1:1 ratio by volume.

2.3.2 Fabrication procedure

The whole fabrication process of the multi-motion soft robot's fabrication process is divided into three parts: Fabricating three overall soft multi-bladder pneumatic actuators by 3D printing technology; fabricating the soft triboelectric tactile sensor; assembling the soft robot. The detail of fabrication procedure of the soft robot is shown in Fig. 7.

The three-dimensional (3D) model of soft robot is designed in SolidWorks, which is a Computer Aided Design (CAD) software package. After the 3D printing software coverd the STL model and generated the movement paths, the soft robot is manufactured by the designed custom 3D printer using viscoelastic silicone material loaded into the syringe. Finally, the manufactured soft robot is cured in humidity environment at 60 ˚C for 24 h and a tube is embedded into the fabricated structure to create the robotic system. The soft tactile sensor is made of silicone rubber (Eco-flex 0050) and liquid metal (E-Galn). The mold used to fabricate the sensor is printed by the 3D printing platform named MakerBot, and then the casting of the silicone and the injection of liquid metal are carried out. After the soft tactile sensor solidified, the wires were connected to the sensor.

In the last part, the PVC board is inserted into the reserved hole at the bottom of the soft actuation after the software robot body and the soft sensor had manufactured. The surface of the multi-motion soft robot body is further coated with silicone rubber (Eco-flex 0050) to ensure the sealing property. Then, the soft triboelectric tactile sensor and rigid barb structure are assembled to the robot's body. Finally, the silicone tube is connected to the multi-motion soft robot.

2.4 Movement patterns

The multi-motion modes soft crawling robot can not only perform linear movement in flat ground, but also perform crossing movement in obstacle environment and climbing movement mode in steps environment, according to the different control patterns.

2.4.1 The linear movement pattern

Driven by pressured gas, the soft crawling robot can achieve a stretched cyclical movement. In Fig. 8a, a cycle of the process is divided into two parts: the inflatable process and deflated process. At the stage of inflation, the air pump inflates the soft robot's body. Due to the expansion of each air bag, the soft robot will bend at a certain degree. A rigid PVC slice is embedded in the bottom plate of the robot's body to take advantage of the inextensibility of the rigid slice, so that the soleplate does not expand during inflation of the airbag and thus produces a corresponding bending movement. Due to the soft robot's body, the barb structure of the front and back base was designed. The front base receives more friction than that of the rear base when the robot body is flexed, so that the rear part of the robot swings forward. At the stage of deflation, the bevel of the rear base is in contact with the ground, the bottom of the front base is separated from the ground, and the friction of the rear base is relatively high at this time, which further enables the soft robot to extend forward. So that the pump periodically inflated and deflated, prompting the soft crawling robot to achieve a prolonged cyclical forward movement in the flat ground.

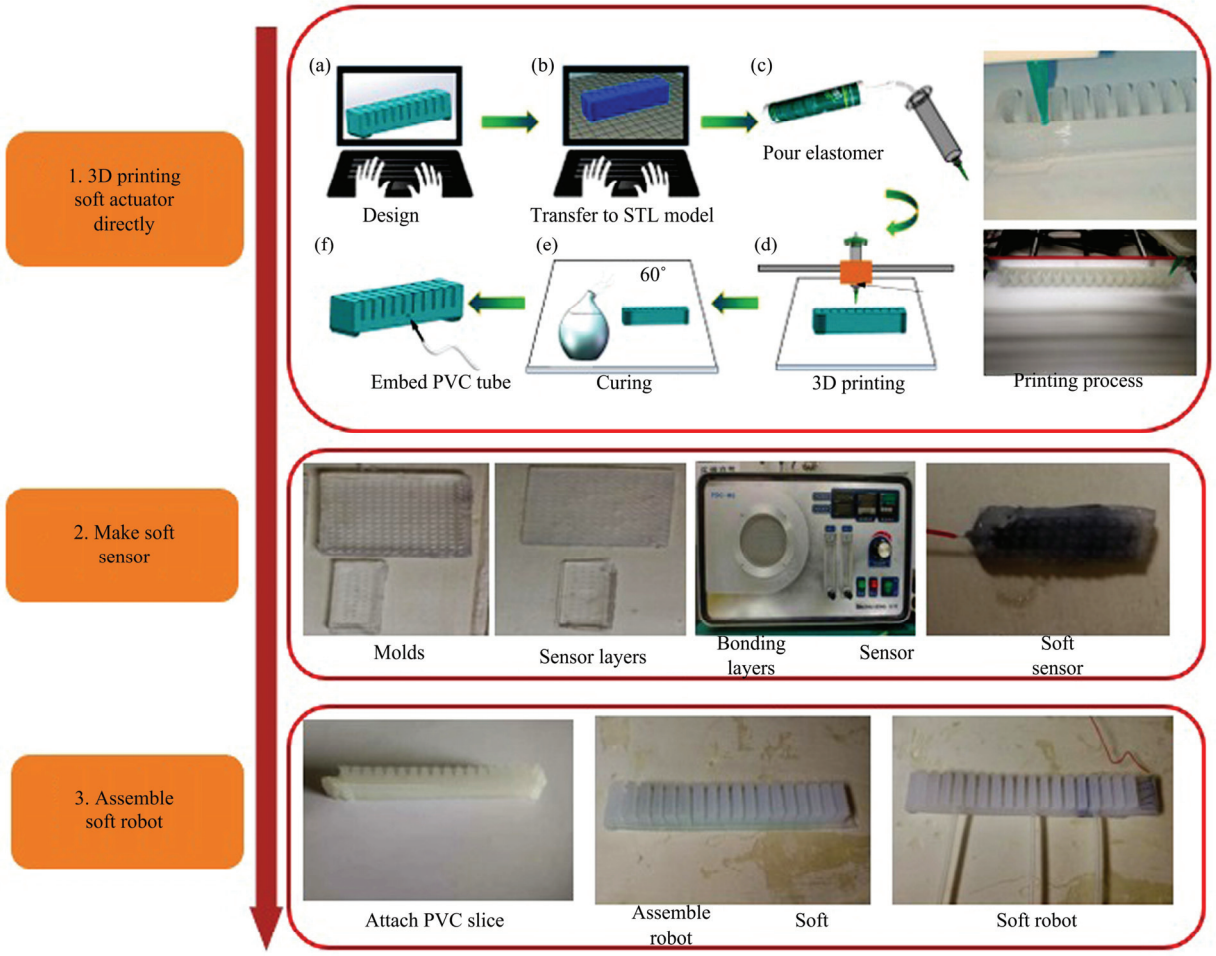

Fig. 7 The soft robot's fabrication process.

2.4.2 The crossing movement pattern

In Fig. 8b, the crossing movement is achieved by the body linear movement, head lift movement and body linear movement after the head lifting. The linear motion of the body of the soft robot has been described. Then we will describe the soft robot's head lift movement and body linear movement after the head lifting. The lifting motion of the head of the soft robot is for avoiding the obstacle encountered by the soft robot in the course of linear motion.

When the head of the soft robot touches the obstacle, the soft sensor attached to the head will send a signal to the control system. Then the control system will control the air pump to pump the pressure air into the head actuator, causing the actuator to bend up. Then the soft robot's body will continue the linear movement. The front feet of the soft robot leaves the ground, and the adhesive tape attached to the bottom of the robot will alternately change the friction during the movement. When the soft robot's head crossed the obstacle, the actuator of the head will return to its initial state.

2.4.3 The climbing movement pattern

The climbing movement is divided into three parts: soft robot's head lift movement, soft robot's body linear movement and soft robot's head linear movement. The soft robot's head lift movement and body linear movements have been described in the upper section. Then we will describe the soft robot climbing movement.

In Fig. 8c, the movement process of the soft robot climbing the first ladder is similar to the crossing movement shown in Fig. 8b. After the soft robot's head is completely resting on the first ladder, the soft robot's head performs the linear movement. The head straight

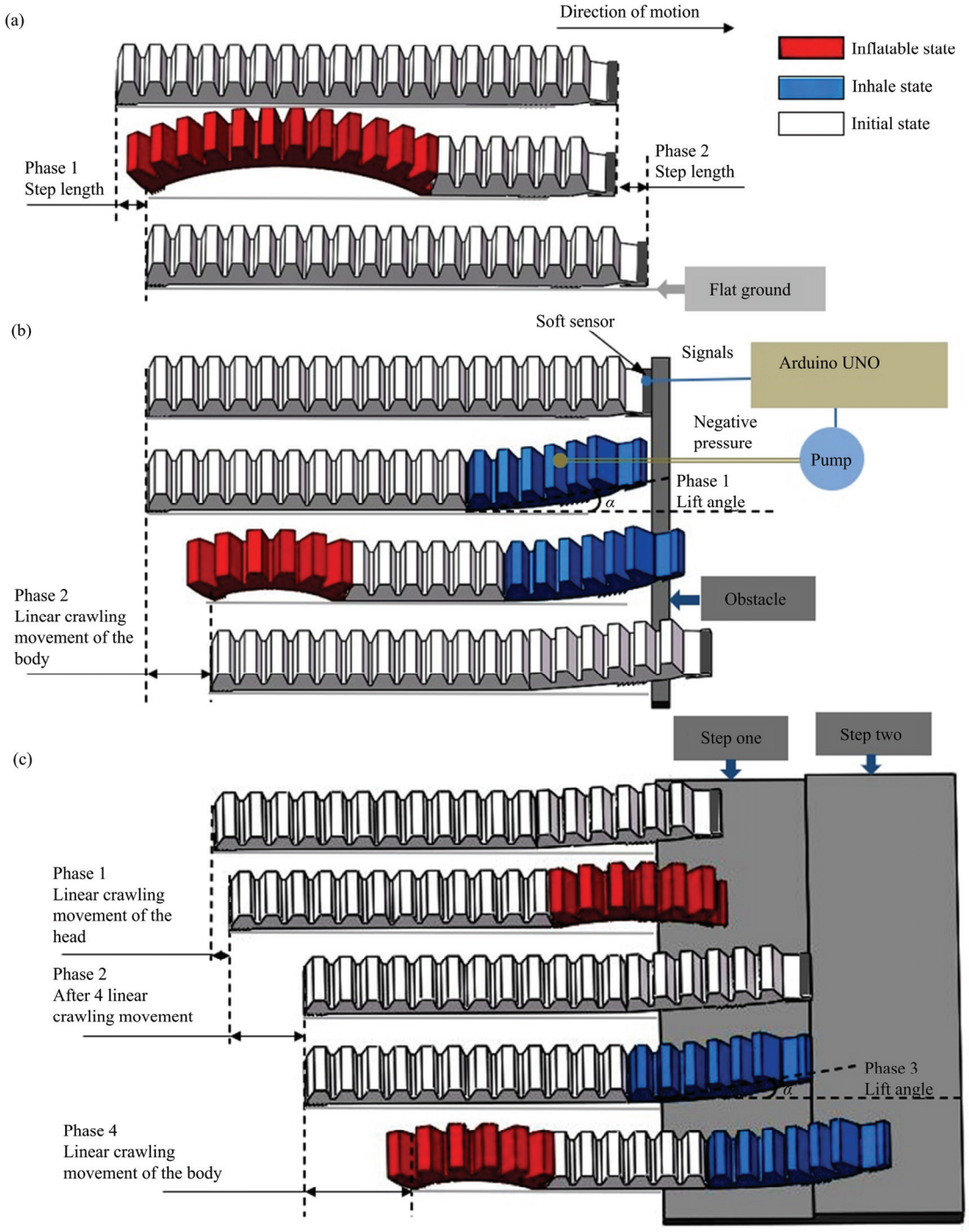

Fig. 8 The different movement patterns of the soft crawling robot under different environments. (a) Flat ground; (b) obstacle; (c) step.

movement is similar to the body straight movement. During the linear movement of the head, the control system will control the air pump to pump pressure air into the head actuator, causing the actuator to bend down. During the inflating process, the front barb will be fixed on the step, and the soft crawling robot's body will move forward due to the swelling and bending of the head actuator. During the deflating process, the rear feet are used as anchors due to the larger static friction force. The front feet move forward with the stretching of the actuators. When the head of the soft robot touches the second ladder, the control system will control the soft

robot's head achieve the lift movement again. Then the soft robot's next steps climbing movement will repeat the above process.

2.5 Control system

Based on the aerodynamic control principle of the soft multi-airbags actuator, we established the closed-loop control system to control the linear movement, including the crossing movement and the climbing movement with the soft sensor. The purpose of the linear movement control is to keep the robot moves in a straight line at the fastest speed. The purpose of the crossing movement control is to keep the robot can cross obstacles in the linear movement. When the robot encounters an obstacle in the course of linear motion, it can cross the obstacle and keep the linear movement. The purpose of the climbing movement control is to keep the soft robot crawling on the steps.

Fig. 9 shows the closed-loop control circuit of the multi-motion modes soft robot, which mainly contains power source (DC12V), air pump, getter pump, reduction valve, electromagnetic valves, microcontrollers (Arduino UNO), electric relay, and the soft robot. We use three independent pneumatic circuits to control the inflation and inhaling of these actuators. Each pneumatic circuit consists of two two-position three-way solenoid valves, two two-position two-way solenoid valves, one inflator pump and one getter pump.

3 Results and discussion

We perform these experiments on the rubber sheet surface, the PVC sheet surface, and the glass surface, respectively, and collect the linear experimental data as shown in Fig. 10. Fig. 11 introduces the experimental process of the linear, crossing and climbing motions. It is done on the PVC sheet surface as an example.

3.1 Linear movement

Fig. 10d shows the soft robot linear motion inflatable control chart, in which the abscissa indicates the inflation time, and ordinate 0 and 1 respectively. During the cyclical exercise test in soft robots, we set inflation time 1 s, and then deflated immediately after the end of the inflatable. After 0.6 s deflation, the robot reaches the initial straight state, and the entire period is 1.6 s.

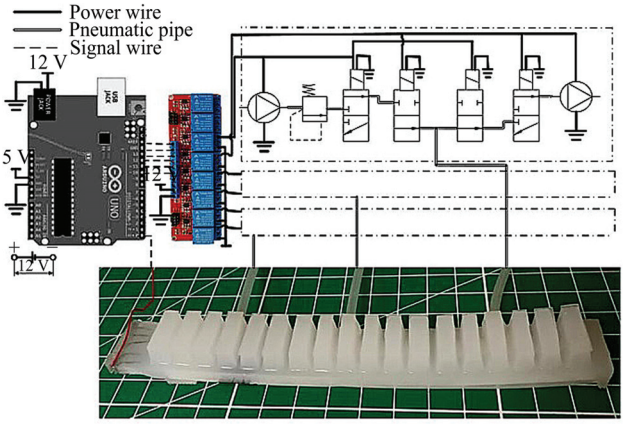

Fig. 9 The closed-loop control circuit of the multi-motion modes soft robot.

To verify the ability of the soft robot to crawl on different material surfaces, the soft robot carried out movements on three different surfaces: the polyvinyl chloride (PVC) plastic (one grid is 10 mm), the rubber sheet, and the glass. The crawl distance "*d*" over a period of time on the different surfaces of the soft robot is shown in Fig. 11.

Fig. 11a shows the linear locomotion process of multi-motion modes soft crawling robot on the PVC plastic surface. The distance of each grid on the experimental platform is about 10 mm. In linear movement experiment, the second and third actuators of the robot body are inflated and deflated synchronously. Fig. 11ai shows the robot at the initial state. Fig. 11bii shows the robot at the inflated state. Fig. 11ciii shows the robot at the deflated state. Under the pressure of 0.6 MPa and other given conditions, the average distance of robot's moving rightward in a cycle is d = 10 mm, and the average moving speed of soft robot is 6.25 mm·s^{-1}. It is mainly to prove that the original basic sports performance can still be maintained after assembling multiple airbags.

3.2 Crossing movement

Fig. 11b shows the crossing motion process of multi-motion modes soft crawling robot on the PVC plastic surface. This experiment is to verify the head automatic lifting ability when encountering obstacles, and the crawling ability of the head after lifting. In this experiment, we place a 100 mm long, 10 mm wide and 5 mm high obstacle, on the robot's crawling path. Fig. 11bi shows the robot at the initial state. Fig. 11bii

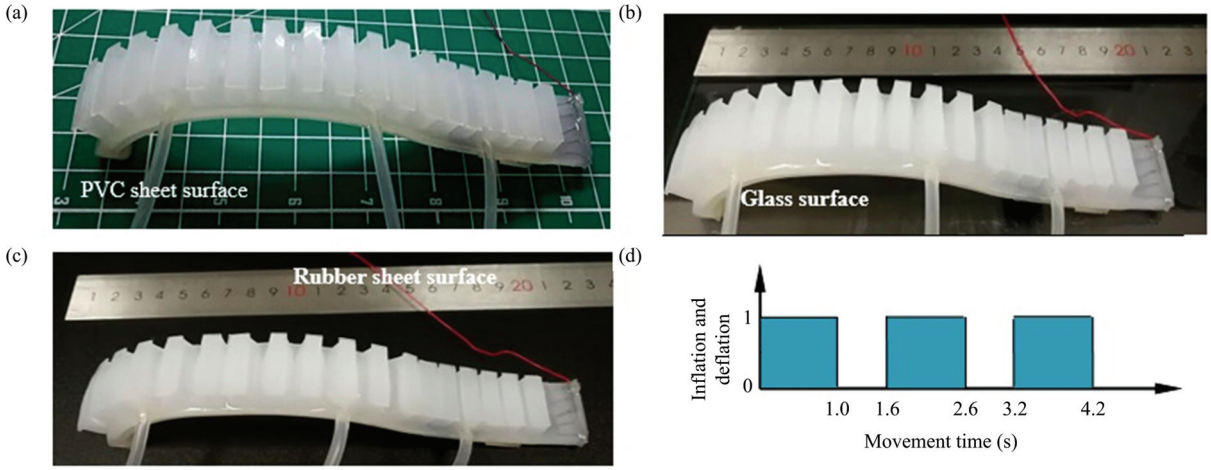

Fig. 10 (a–c) The motion modes of soft robot on three different surfaces and (d) sequence of inflation and deflation.

shows the inhaled process of the first actuator when the head touches the obstacle. At this process, the bending up of the first actuator is caused by the inhaled of the getter pump. Fig. 11biii shows the inflated process of the second and third actuator when the soft robot's head has lifted. The Fig. 11biv shows the deflated process of the second and third actuator. Fig. 11bv shows the final state after the whole crossing movement process.

3.3 Climbing movement

Fig. 11c shows the climbing motion process of multi-motion modes soft crawling robot on the steps surface. This experiment is to verify the soft robot's climbing ability of the soft robot when the robot crawl stairs. In this experiment, we set a two-storey step with a height of 5 mm to test the ability of the soft robot climbing the steps. Fig. 11ci shows the robot at the initial state. Fig. 11cii shows the inhaled process of the first actuator when the actuator touches the first ladder. Fig. 11ciii shows the inflated process of the second and third actuators when the soft robot's head has lifted. Fig. 11civ shows the deflated state of the second and third actuators after 3 times linear movement of the soft robot's body. The Fig. 11cv shows the head has completely rested on the first ladder. Figs. 11cvi and 11cvii show the linear movement of the soft robot's head. The Figs. 11cviii and 11cix show the next climbing movement process of the second ladder.

The above experimental results show that the multi-motion mode soft robot can successfully complete the crawling motion in a flat environment, the leapfrog motion in an obstacle environment, and the climbing motion in a ladder environment under the control of a closed-loop system. It verifies the adaptability of the soft robot in a complex environment.

4 Conclusion

In this article, a multi-motion modes soft crawling robot is designed and fabricated. It is composed of three soft multi-bladder actuators, one soft sensor, middle layer, bottom layer, front feet, front barb, and rear feet. This robot can perform multi-motion, according to the different positive or negative pressure control of three soft multi-bladder actuators. Linear movement pattern, crossing movement pattern and climbing movement pattern are presented. We establish the closed-loop automatic control system, which use soft sensor to control the soft robot pass through the complex environment. According to the experiment, this linear motion model can keep the robot moving toward the same direction, and the average speed of the linear locomotion is 6.25 mm·s^{-1} on the PVC surface. In the above experimental condition, the crossing obstacle movement model has a high accuracy rate, and after fifteen cycles of movement, the soft robot can pass through an obstacle. In the above experimental condition, the climbing movement is composed of the linear movement and crossing movement, the soft robot climb up multiple stairs by alternating linear motion with spanning motion. Finally, the ability of a soft robot to traverse complex

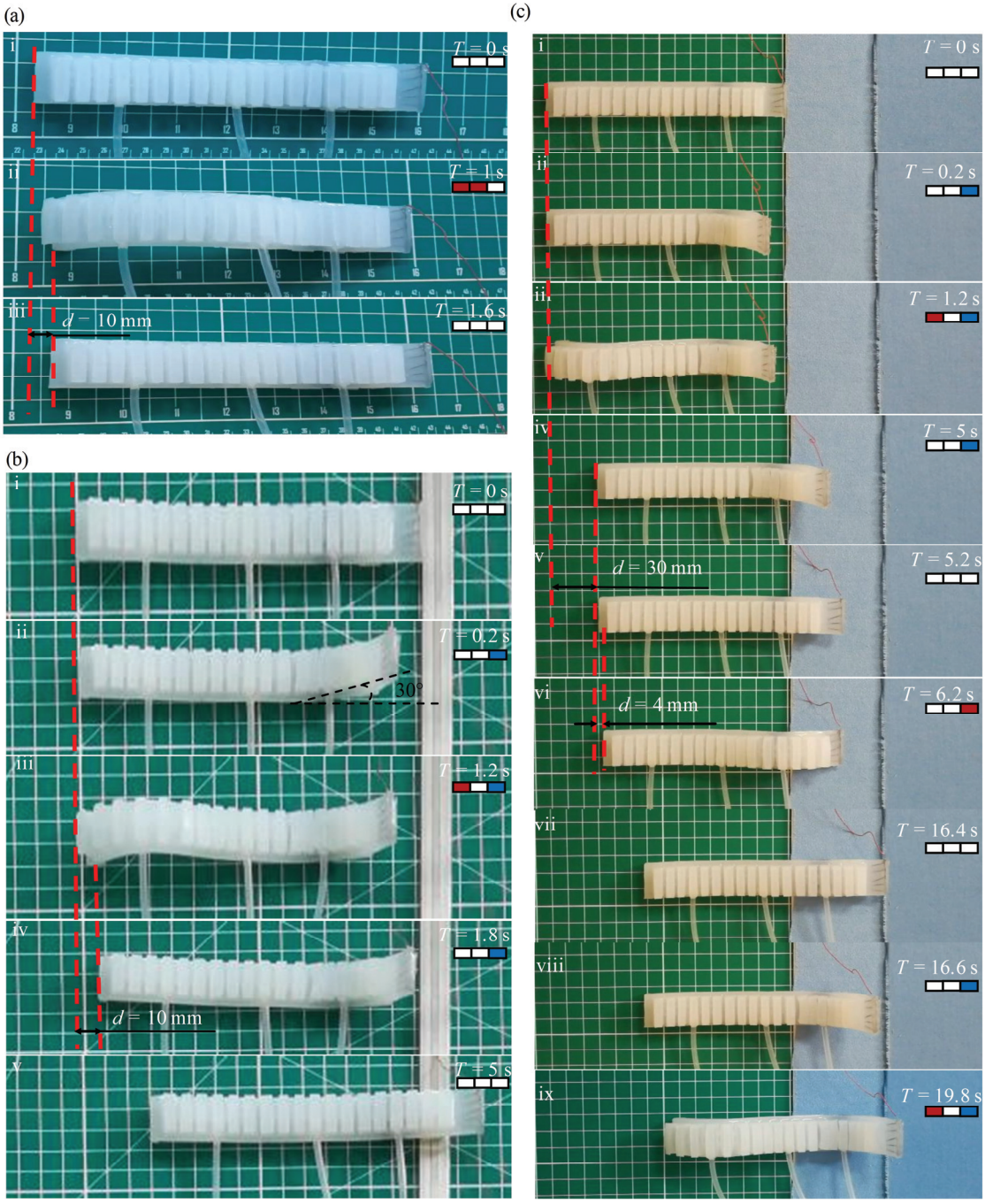

Fig. 11 The movement experiments of the soft crawling robot. (a) Flat ground; (b) obstacle; (c) step.

environments is verified by the complex environments experiment under the closed-loop automatic control system.

Acknowledgment

This work was supported by National Natural Science Foundation of China (Grant No. 61773274).

References

[1] Laschi C, Mazzolai B, Cianchetti M. Soft robotics: Technologies and systems pushing the boundaries of robot abilities. *Science Robotics*, 2016, **1**, eaah3690.

[2] Rus D, Tolley M T. Design, fabrication and control of soft robots. *Nature*, 2015, **521**, 467–475.

[3] Wang W, Lee J Y, Rodrigue H, Song S H, Chu W S, Ahn S H. Locomotion of inchworm-inspired robot made of smart soft composite (SSC). *Bioinspiration & Biomimetics*, 2014, **9**, 046006.

[4] Kim H J, Song S H, Ahn S H. A turtle-like swimming robot using a smart soft composite (SSC) structure. *Smart Materials & Structures*, 2011, **22**, 014007.

[5] Wehner M, Truby R L, Fitzgerald D J, Mosadegh B, Whitesides G M, Lewis J A. An integrated design and fabrication strategy for entirely soft autonomous robots. *Nature*, 2016, **536**, 7617.

[6] Jin H, Dong E B, Xu M, Liu C S, Alici G, Jie Y. Soft and smart modular structures actuated by shape memory alloy (SMA) wires as tentacles of soft robots. *Smart Materials & Structures*, 2016, **25**, 085026.

[7] Wang Y P, Yang X B, Chen Y F, Wainwright D K, Kenaley C P, Gong Z Y, Liu Z M, Liu H, Guo J, Wang T M, Weaver J C, Wood R J, Wen L. A biorobotic adhesive disc for underwater hitchhiking inspired by the remora suckerfish. *Science Robotics*, 2017, **2**, eaan8072.

[8] Shintake J, Rosset S, Schubert B, Floreano D, Shea H. Versatile soft grippers with intrinsic electroadhesion based on multifunctional polymer actuators. *Advanced Materials*, 2016, **28**, 231–238.

[9] Mao S X, Dong E B, Jin H, Xu M, Zhang S W, Yang J, Low K H. Gait study and pattern generation of a starfish-like soft robot with flexible rays actuated by SMAs. *Journal of Bionic Engineering*, 2014, **011**, 400–411.

[10] Morales D, Palleau E, Dickey M D, Velev O D. Electro-actuated hydrogel walkers with dual responsive legs. *Soft Matter*, 2014, **10**, 1137–1148.

[11] Umedachi T, Trimmer B A, Design of a 3D-printed soft robot with posture and steering control. *IEEE International Conference on Robotics and Automation* (*ICRA*), Hong Kong, 2014, 2874–2879.

[12] Wang W, Lee J Y, Rodrigue H, Song S H, Chu W S. Locomotion of inchworm-inspired robot made of smart soft composite (SSC). *Bioinspiration & Biomimetics*, 2014, **9**, 046006.

[13] Shepherd R F, Ilievski F, Choi W, Morin S A, Stokes A A, Mazzeo A D. Multigait soft robot. *Proceedings of the National Academy of Sciences of the United States of America*, 2011, **108**, 20400–20403.

[14] Guo H X, Zhang J H, Wang T, Li Y J, Hong J, Qiu L. Design and control of an inchworm-like soft robot with omega-arching locomotion. *IEEE International Conference on Robotics and Automation*, Singapore, Singapore, 2017, 4154–4159.

[15] Hu B B, Jin G Q. Design and fabrication of a multi-actuator soft robot inspired by young tiger beetle. *Jiqiren*/*Robot*, 2018, **40**, 626–633.

[16] Duduta M, Clarke D R, Wood R J. A high speed soft robot based on dielectric elastomer actuators. *IEEE International Conference on Robotics and Automation*, Singapore, Singapore, 2017, 4346–4351.

[17] Nakamaru S, Maeda S, Hara Y, Hashimoto S. Development of novel self-oscillating gel actuator for achievement of chemical robot. *IEEE*/*RSJ International Conference on Intelligent Robots and Systems*, St. Louis, MO, USA, 2009, 4319–4324.

[18] Shi Z Y, Pan J , Tian J W, Huang H, Jiang Y R, Zeng S. An inchworm-inspired crawling robot. *Journal of Bionic Engineering*, 2019, **16**, 582–592.

[19] Wu P, Wang J B, Fei Y Q. The structure, design, and closed-loop motion control of a differential drive soft robot. *Soft Robotics*, 2018, **5**, 71–80.

[20] Yeo O H. Some forms of the strain energy function for rubber. *Rubber Chemistry and Technology*, 1993, **66**, 754–771.

[21] Elsayed Y, Vincensi A, Lekakou C, Tao G. Finite element analysis and design optimization of a pneumatically actuating silicone module for robotic surgery applications. *Soft Robotics*, 2014, **1**, 255–262.

[22] Tian X Q, Plott J, Wang H J, Zhu B Z, Shih A J. Silicone foam additive manufacturing by liquid rope coiling. *Procedia CIRP*, 2017, **65**, 196–201.